Calibration of a Thomson parabola ion spectrometer and Fujifilm imaging plate detectors for protons, deuterons, and alpha particles

C. G. Freeman,[1] G. Fiksel,[2] C. Stoeckl,[2] N. Sinenian,[3] M. J. Canfield,[1] G. B. Graeper,[1] A. T. Lombardo,[1] C. R. Stillman,[1] S. J. Padalino,[1] C. Mileham,[2] T. C. Sangster,[2] and J. A. Frenje[3]

[1]*Physics Department, SUNY Geneseo, Geneseo, New York 14454, USA*
[2]*Laboratory for Laser Energetics, University of Rochester, Rochester, New York 14623, USA*
[3]*Plasma Science and Fusion Center, Massachusetts Institute of Technology, Cambridge, Massachusetts 02139, USA*

(Received 16 March 2011; accepted 10 June 2011; published online 8 July 2011)

A Thomson parabola ion spectrometer has been designed for use at the Multiterawatt (MTW) laser facility at the Laboratory for Laser Energetics (LLE) at the University of Rochester. This device uses parallel electric and magnetic fields to deflect particles of a given mass-to-charge ratio onto parabolic curves on the detector plane. Once calibrated, the position of the ions on the detector plane can be used to determine the particle energy. The position dispersion of both the electric and magnetic fields of the Thomson parabola was measured using monoenergetic proton and alpha particle beams from the SUNY Geneseo 1.7 MV tandem Pelletron accelerator. The sensitivity of Fujifilm BAS-TR imaging plates, used as a detector in the Thomson parabola, was also measured as a function of the incident particle energy over the range from 0.6 MeV to 3.4 MeV for protons and deuterons and from 0.9 MeV to 5.4 MeV for alpha particles. The device was used to measure the energy spectrum of laser-produced protons at MTW. © *2011 American Institute of Physics*. [doi:10.1063/1.3606446]

I. INTRODUCTION

A Thomson parabola ion spectrometer (TPIS) is a device used to measure the charge-to-mass ratio and the energy spectra of charged ions. This device has found applications in studying the acceleration of ions by ultra-intense lasers.[1–4] Similar devices have been used in magnetic fusion research.[5] The device described in this paper was designed for the Multiterawatt (MTW) laser facility[6–8] at the Laboratory for Laser Energetics (LLE).

In a TPIS, parallel magnetic and electric fields are used to deflect ions of a given charge-to-mass ratio onto unique parabolic curves at the detector plane.[9] The magnetic dispersion is proportional to the charge-to-momentum ratio and is perpendicular to the electric dispersion, which is proportional to the charge-to-energy ratio. Once calibrated, the position of the ions on the detector plane can be used to determine the ion energy. The number of ions detected at each position can be used to determine the ion energy spectrum.

The main results contained in this paper are: (1) A robust and efficient design of a Thomson parabola ion spectrometer is described. Its small size, ease of fabrication and operation, and low cost makes it attractive even for small-size laboratories. (2) The spatial dispersion (both electric and magnetic) of the device was absolutely calibrated using ion beams from the SUNY Geneseo 1.7 MV tandem Pelletron accelerator. (3) The sensitivity of Fujifilm imaging plates (IP), used as a detector in the device, was measured as a function of energy for protons, deuterons, and alpha particles from the SUNY Geneseo Pelletron accelerator. (4) The device was used to measure the energy spectrum of laser-produced protons at the MTW facility.

II. DESIGN AND OPERATION

There has been much interest in studying ions that are accelerated from the rear side of targets illuminated with ultra-intense ($\gtrsim 10^{19}$ W/cm^2) laser light. The target-normal sheath acceleration mechanism has been proposed to describe the process by which these ions are accelerated.[10] The ultra-intense laser light produces hot electrons in the front of the target that exit on the rear side of the target foil. This causes electric fields of the order of teravolts per meter to be produced behind the target.[11] Atoms on the rear side of the target surface are ionized and these ions are accelerated normal to the target by the strong electric field. Protons, usually present on the target surface in a thin layer from hydrocarbon or water contaminants, are preferentially accelerated due to their high charge-to-mass ratio. Maximum proton energies of tens of MeV are typical. Other ions can be accelerated by this mechanism. Possible applications of such laser-accelerated ion beams include medical proton therapy, fast ignition, and traditional accelerator injectors.[12,13]

A Thomson parabola ion spectrometer has been constructed for the Multiterawatt laser facility. The MTW peak intensity was expected to produce laser-accelerated protons with energies of up to 20 MeV. The TPIS was designed to provide energy resolution of better than 10% for 20 MeV protons, while allowing more than 10^5 protons to enter the device. The design requirements could be met with a compact device based on a permanent magnet and a pair of electrostatic deflector plates to produce the fields necessary to deflect the incident ions. A schematic of the diagnostic is shown in Fig. 1. The particles enter the diagnostic through a 400 μm diameter tantalum pinhole aperture. The aperture is mounted in

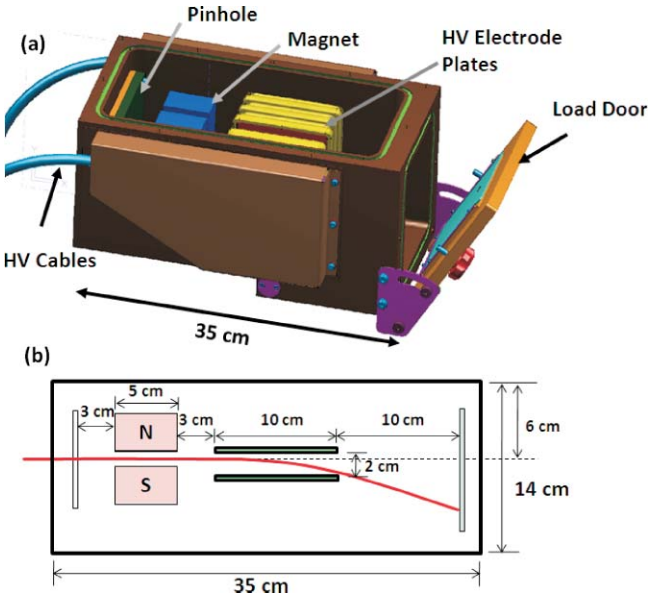

FIG. 1. (Color online) Schematic of the Thomson parabola ion spectrometer that was built for use at the Multiterawatt laser facility at LLE. Figure (a) shows a CAD model of device. Figure (b) is a top-view schematic showing key dimensions.

a tungsten plate that provides shielding from incident x rays. The aperture size affects the energy resolution and the number of protons that enter the TPIS. The design allows the aperture to be easily replaced so that the balance between energy resolution and number of incident ions can be adjusted. The permanent magnet (from Dexter Magnetics[14]) is located 3 cm behind the entrance aperture and has a pole gap of 1 cm and a length of 5 cm. This magnet has a maximum field strength of 0.53 T. The electrostatic deflector plates are made of highly polished stainless steel and are 10 cm long with a separation of 2 cm. These plates are mounted on insulating standoffs made of Ultem™,[15] which are specially shaped to prevent electrical breakdown. Each electrostatic deflector plate is connected to a standard commercial high voltage power supply;[16] one of positive polarity and the other negative. The maximum potential on each power supply is 40 kV, which yields a maximum electric field of 40 kV/cm. A turbo pump is mounted on the top of the diagnostic so that the TPIS can be independently evacuated to pressures less than 10^{-5} Torr.

A load door on the back of the diagnostic allows a variety of particle detectors to be inserted in the device. Radiochromic film, plastic nuclear track detector CR-39, and Fujifilm imaging plates[17] have all been fielded on this diagnostic. The use of imaging plates to detect the incident ions has several advantages. Imaging plates are easily scanned using a commercial scanner (Fujifilm BAS 1800-II) which gives a photo-stimulated luminescence (PSL) value for each pixel, with a maximum spatial resolution of 50 μm by 50 μm. In addition, the imaging plates' response function has been shown[18] to be linear over a wide range and they are reusable, which make these detectors very attractive for use in a Thomson parabola diagnostic.

III. SPATIAL DISPERSION CALIBRATIONS

The electric and magnetic deflections of the TPIS were calibrated using monoenergetic proton and alpha particle beams from the SUNY Geneseo 1.7 MV tandem Pelletron accelerator. The accelerator is a model 5SDH from the National Electrostatics Corporation.[19] A negative ion beam with a charge of -1 is produced in the RF alkali charge exchange ion source and is accelerated to the high voltage terminal, which is located in the center of the accelerator. Inside the terminal, the ion beam passes through a stripper canal which is filled with a low pressure nitrogen gas. As the ions pass through the stripper canal, a fraction of these ions lose more than one of their electrons and become positively charged. These positive ions then get another stage of acceleration as they exit the high voltage terminal. The maximum energy that can be produced is given by $(Q+1)V$, where Q is the integral charge state of the ion as it exits the stripper gas in the terminal and V is the potential on the terminal. For protons, the maximum energy is therefore 3.4 MeV, and for alpha particles the maximum energy is 5.4 MeV. The voltage ripple on the high voltage terminal is less than 200 V rms and is measured with a capacitive pick-off.

The magnetic field of a dipole magnet at the exit of the accelerator is set to deflect ions of a particular energy and charge state down a beamline that is oriented at a 30° angle with respect to the accelerator axis. The Thomson parabola was mounted on the end of a cylindrical 70 cm diameter scattering chamber at the end of this beamline, as shown in Fig. 2.

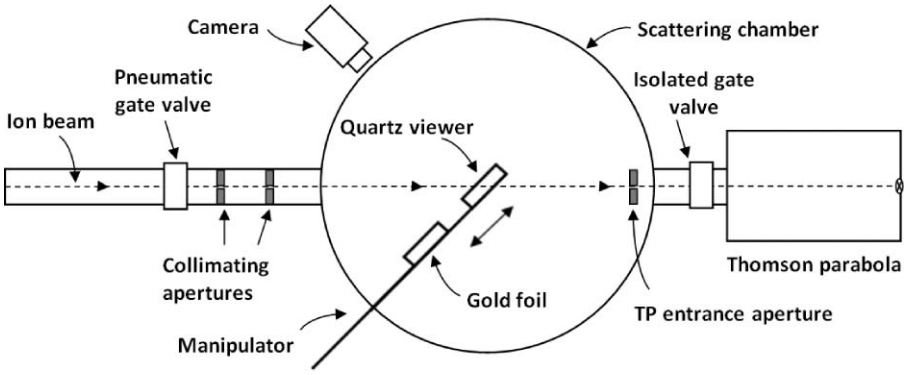

FIG. 2. Schematic of the experimental setup at the SUNY Geneseo Pelletron accelerator. The magnetic deflection of the Thomson parabola is into the page and the electric deflection is toward the bottom of the page.

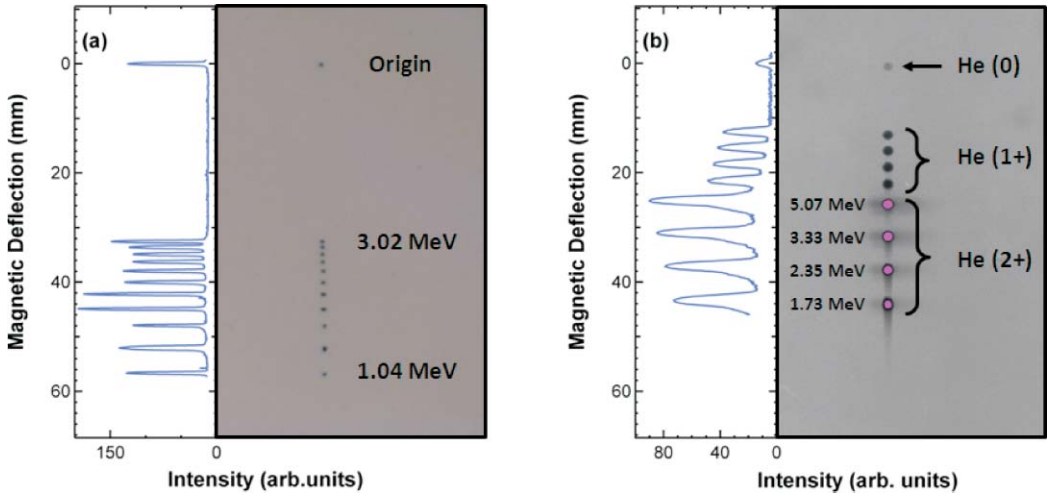

FIG. 3. (Color online) Thomson parabola magnetic position calibrations. Figure (a) shows proton data, in which radiochromic film was used on the detector plane. Figure (b) shows alpha particle data, in which Fujifilm imaging plate was used on the detector plane. Note that for a given exposure at a given energy, both the 1+ and 2+ charge states of helium-4 are clearly visible.

The TPIS was aligned using a laser which was directed down the beamline. A magnetically coupled manipulator, oriented at 45° with respect to the beam axis, was used to position either a quartz beam viewer or thin (0.1 μm) gold foil in the chamber.

A. Magnetic deflection calibration

The procedure for carrying out the Thomson parabola magnetic field calibration measurements is described below. The quartz beam viewer was positioned in the center of the scattering chamber. The ion beam profile on the quartz was inspected visually using a camera mounted on a viewport perpendicular to the quartz viewer. The beam was tuned so that it made a small, uniform beam spot on the quartz viewer. Then the manipulator was repositioned so that the beam was incident on the gold foil. The isolated gate valve was then opened, and the pneumatic gate valve at the entrance to the scattering chamber was shuttered open and closed to provide a short (≈1 s) exposure of the detector. Precise control of the exposure time was not important since the purpose of these measurements was to measure the deflection of the ions. The beam spot on the gold foil served as an object for an effective pinhole camera formed by the TPIS entrance aperture and detector plane. For the position measurements, both Gafchromic HD-810 radiochromic film (for the protons) and Fujifilm BAS-TR imaging plates (for the alpha particles) were used to detect the ions at the rear of the TPIS. The TPIS electrostatic deflectors were not used for this part of the experiment. As the alpha particles pass through the gold foil, a fraction of them emerge in the neutral, 1+ and 2+ charge states. Each of these charge states is deflected by a different amount by the TPIS magnet. The neutral helium-4 atoms are used to define the zero point for the calibration. For the proton measurements, a separate shot was performed without the magnet in place to establish the origin.

After exposure, the imaging plates were scanned using a Fujifilm BAS-1800-II reader, and the radiochromic film was scanned using an Epson 10000 XL scanner.[20] The results of these scans are shown in Fig. 3. A line-out of each scan was performed (also shown in Fig. 3) and each peak in the distribution was fit with a Gaussian to determine the centroid. Since the magnetic deflection is proportional to the charge-to-momentum ratio, a plot of magnetic deflection versus $q/\sqrt{m \cdot KE}$ was made, where q is the charge of the ion, m is its mass, and KE is its kinetic energy. Figure 4 shows the results of this plot. The black line represents a linear least-squares fit to the data. The slope of this line is 57.79 ± 0.23 mm MeV$^{1/2}$ amu$^{1/2}/e = (5.883 \pm 0.023) \times 10^{-3}$ Wb. Using the small angle approximation, the magnetic deflection can be approximated by

$$x_m = \frac{q \cdot \int B\, d\ell}{\sqrt{2 \cdot m \cdot KE}} \left(D_1 + \frac{d_1}{2} \right), \tag{1}$$

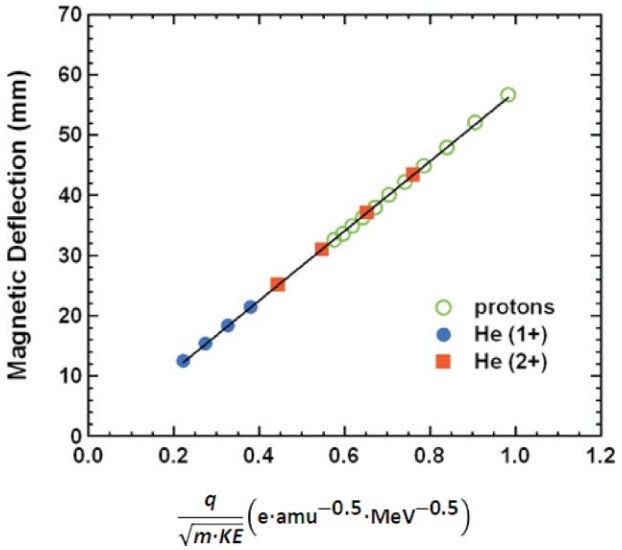

FIG. 4. (Color online) Thomson parabola magnetic field deflection calibration results.

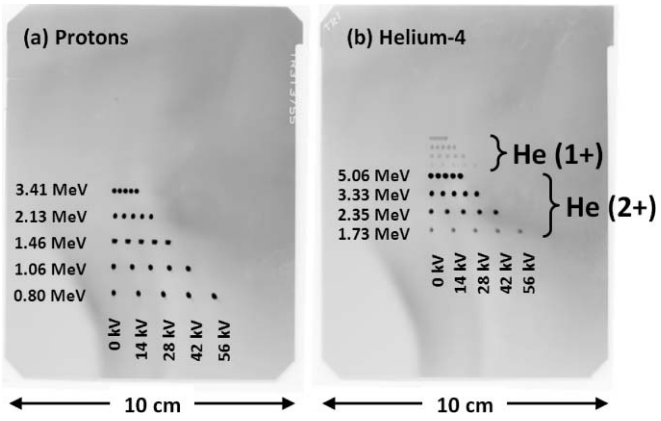

FIG. 5. Electric field deflection calibration for (a) protons and (b) helium-4 ions. The electric deflection is horizontal and the magnetic deflection is vertical. The potential difference across the electrostatic deflectors was varied from 0 to 56 kV in steps of 14 kV. After the alpha particles pass through the gold foil, multiple charge states of helium-4 emerge from the foil. The 1+ charge state is barely visible in the figure.

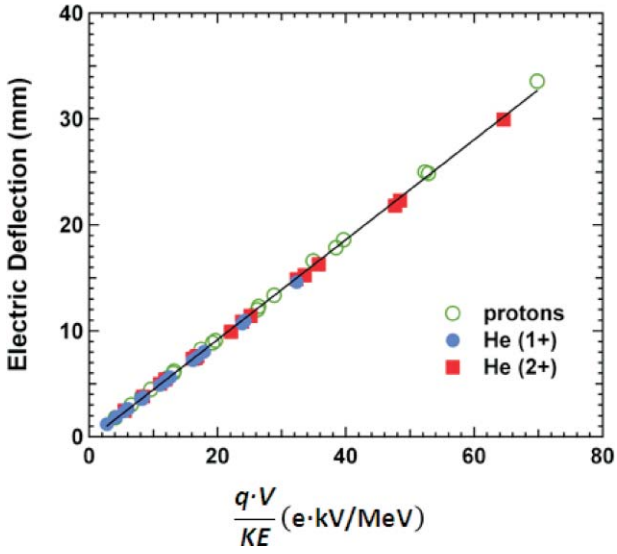

FIG. 6. (Color online) Thomson parabola electric field deflection calibration results.

where d_1 is the length of the magnet and D_1 is the magnet drift length (the distance from the exit of the magnet to the detector plane). The integral of the component of the magnetic field perpendicular to the pole face through the magnet is given by $\int B\, d\ell$ and was estimated from magnetic field data supplied by the magnet manufacturer. The theoretical slope of the line in Fig. 4 is given by

$$\frac{\int B\, d\ell}{\sqrt{2}}\left(D_1 + \frac{d_1}{2}\right) = 53.28\ \text{mm MeV}^{1/2}\,\text{amu}^{1/2}/e = 5.424 \times 10^{-3}\ \text{Wb}, \quad (2)$$

which agrees with the measured slope of the data to within 8%.

B. Electric deflection calibration

The electric field position calibration was also carried out using proton and alpha particle beams from the Pelletron accelerator. For these measurements, imaging plates were used to detect the ions. The potential difference across the electrostatic deflector plates was varied from 0 to 56 kV in steps of 14 kV. Five different energies from 0.80 to 3.41 MeV were used for protons and four different energies from 1.73 MeV to 5.06 MeV were used for the alpha particles. Figure 5 shows the output from the imaging plates for these measurements. The electric deflection is horizontal and the magnetic deflection is vertical. As described earlier, a line-out of the image plate scans was made and the peaks were fit with a Gaussian to determine their centroids. Since the electric deflection is proportional to the field strength and the charge-to-energy ratio, a plot was made of the electric deflection versus $q \cdot V/KE$, where q is the charge of the incident ion and V is the potential difference across the HV electrodes. These results are shown in Fig. 6. The straight line in the figure is the result of a linear least-squares fit to the data. The slope of this line is 0.4723 ± 0.0021 mm MeV/e kV $= 0.4723 \pm 0.0021$ m. Using the small angle approximation, the electric deflection can be approximated as

$$x_e = \frac{q \cdot \int E\, d\ell}{2 \cdot KE}\left(D_2 + \frac{d_2}{2}\right), \quad (3)$$

where d_2 and D_2 are the electrode length and electric drift length, respectively. The integral of the component of the electric field perpendicular to the electrostatic deflector plates through the midplane is $\int E\, d\ell$. This integral was estimated numerically using the finite element analysis software package FEHT (Ref. 21) and gave a result that was 20% larger than the ideal parallel-plate capacitor case, i.e., $\int E\, d\ell = 1.20\ V\, d_2/\delta$, where δ is the distance between the high voltage electrodes. Therefore, the theoretical slope of the data shown in Fig. 6 is

$$1.20\frac{d_2}{\delta}\left(D_2 + \frac{d_2}{2}\right) = 0.450\ \text{m}, \quad (4)$$

which agrees with the measured value to within 5%.

IV. IP RESPONSE CALIBRATIONS AND MTW PROTON SPECTRUM

The response of Fujifilm BAS-TR imaging plate detectors was measured for protons, deuterons, and alpha particles. Such a calibration is necessary for absolute ion energy spectra to be determined from the TPIS when imaging plates are used. The experimental setup used for the IP response calibrations was similar to that used in the position calibrations described in Sec. III. The entrance aperture was electrically isolated and was connected to a digital electrometer. Another digital electrometer was connected to the isolated gate valve.

The procedure for these measurements was as follows. The quartz viewer was initially placed in the center of the chamber and was used to visually inspect the beam profile. The beam was tuned so that the beam profile on the quartz was roughly elliptical, with the long axis in the vertical direction. The horizontal width of the beam was reduced to ensure that the ions entering the Thomson parabola passed

straight through the magnet poles without scattering off the magnet surface. Once the desired spatial beam profile had been achieved, the quartz viewer was replaced by the gold foil. Prior to each shot, with the isolated gate valve closed, the ratio of the beam current on the entrance aperture to the beam current on the isolated gate valve was measured. The isolated gate valve with an attached coupling nipple acted as an insertable Faraday cup, and the length of this cup (length-to-diameter ratio = 5.4) made for efficient capture of the secondary emission electrons. After the beam current ratio was measured, the pneumatic gate valve at the entrance to the scattering chamber was closed and the isolated gate was opened. The digital electrometer on the entrance aperture was put into charge mode, so that the total integrated beam current incident upon it could be measured. The pneumatic gate valve was then shuttered open and closed, with an exposure time of ~0.8 s. Precise control of the exposure time was not necessary, since the number of ions for each shot was determined from the accumulated charge on the TP entrance aperture. Following the exposure, the TPIS was then vented and the imaging plate was removed and placed on the Fujifilm BAS-1800 II imaging plate reader. Because the PSL value of an exposed imaging plate tends to decay with time, each scan was started 7 min after the exposure. Each scan was inspected to ensure that there was no saturation of the imaging plate and that the incident ion beam was not clipped by striking the magnet poles in the Thomson parabola. The imaging plate reader software was used to determine the net photo-stimulated luminescence of the beam spot and the background was subtracted. The net PSL value was divided by the total number of incident ions to achieve the figure-of-merit, which is the PSL per particle.

For the low energy alpha particle ion shots, multiple charge states were observed exiting the gold foil. Each of the charge states were easily separated after passing through the magnet in the Thomson parabola and could be counted independently on the IP. Assuming the response of the imaging plates is independent of the incident charge state, a measurement of the net PSL in each charge state allowed the charge state fractions to be determined. This in turn allowed the total number of particles incident on the imaging plates to be determined from measurements of the net charge entering the device.

Figure 7 shows the photo-stimulated luminescence per particle as a function of energy. Three different ions are shown here; protons, deuterons, and alpha particles. After the helium-4 ions pass through the stripper canal in the center of the terminal, some of them emerge in the 2+ charge state and some emerge in the 1+ charge state. The dipole magnet at the exit of the accelerator can be set to send either the 2+ or the 1+ ions down the beamline to the scattering chamber. Most of the data points obtained for helium-4 ions were for the 2+ charge state, but to check the reproducibility of the data one additional experiment was performed in which the dipole magnet was set to direct the He (1+) ions into the scattering chamber. This point is represented by the black "X" in Fig. 7 and it is in good agreement with the rest of the He (2+) data.

The positions of the maxima in the IP response curves were compared to calculations of the minimum energy required for a particular ion species to completely pass through the active layer of the IP. The thickness and composition of the active layer were obtained from Fujifilm,[22] and the program SRIM (Ref. 23) was used to perform the calculations. The punch-through energies for protons and deuterons determined from SRIM (1.5 MeV and 2.0 MeV, respectively) can be compared to the peaks in the PSL/particle sensitivity curves shown in Fig. 7. The punch-through energy for alpha particles is 7.0 MeV and is higher than the maximum achievable alpha particle energy from the accelerator. For incident ions with energies below the punch-through energy, the ions will deposit all of their energy in the sensitive layer of the imaging plate. The observed difference in IP sensitivity for protons, deuterons, and alpha particles for energies below 1.5 MeV (the minimum punch-through energy, for the protons) may indicate that the IP sensitivity depends not only on the total energy deposited in the active layer but also the stopping power (dE/dx) of the incident ion.

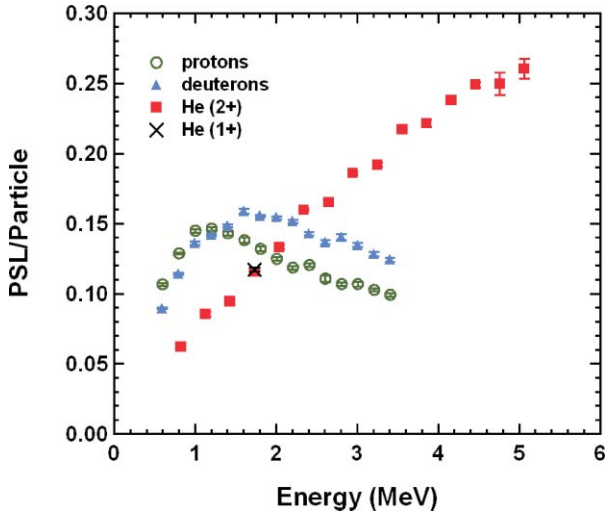

FIG. 7. (Color online) Photo-stimulated luminescence per particle of Fujifilm BAS-TR imaging plates as a function of particle energy.

The response of imaging plates to protons of various energies reported here has a similar shape to the data reported previously in laser-based experiments;[24,25] however, the IP sensitivity reported here is 8%–37% lower than reported in Ref. 24. Part of this discrepancy may be due to IP fading effect and/or differences in IP reader sensitivity. The current work complements and extends on the previous experiments by including IP sensitivity for both deuterons and alpha particles. The principal difference is that the measurements reported here are made using monoenergetic beams from an accelerator rather than ions produced in ultra-intense laser-matter interactions.

The Thomson parabola has been fielded on MTW and absolutely calibrated proton energy spectra have been obtained for various target foils and laser energies. Figure 8 shows a proton energy spectrum for a 8.1 J laser pulse with duration of 1.3 ps incident on a 500 μm × 500 μm square copper foil of thickness 20 μm. The PSL values from the IP were converted into number of protons using the sensitivity curve shown in Fig. 7. Although proton energies up to 20 MeV were observed, the proton energy spectrum shown in Fig. 8 has

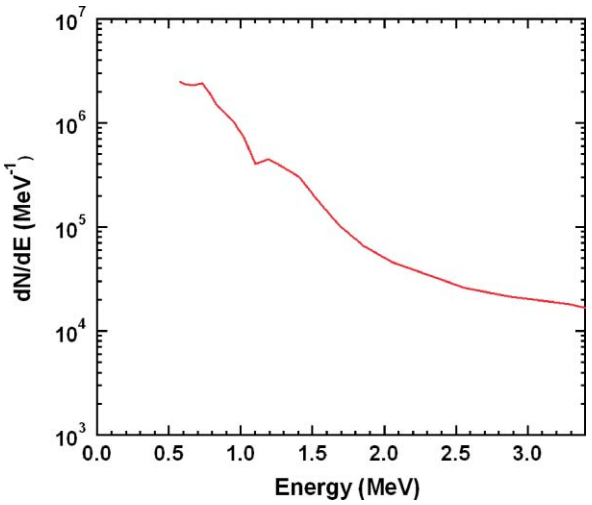

FIG. 8. (Color online) Absolutely calibrated proton energy spectrum obtained using Thomson parabola with imaging plates on MTW. Although proton energies up to 20 MeV were observed in this experiment, the spectrum shown here extends to 3.4 MeV, which is the maximum proton energy for which the sensitivity of the IP was measured.

been restricted to an upper limit of 3.4 MeV, which is the highest proton energy for which the IP response was absolutely calibrated.

V. CONCLUSIONS/SUMMARY

A Thomson parabola ion spectrometer has been designed to study ions accelerated from the rear side of laser illuminated targets at the LLE Multiterawatt laser facility. The magnetic and electric deflection of the device has been calibrated using ions of well-known energy from the 1.7 MV tandem Pelletron accelerator at SUNY Geneseo, allowing the absolute energy of incident ions to be determined. Furthermore, the sensitivity of Fujifilm imaging plates, used as a detector in the Thomson parabola, has also been measured for protons, deuterons, and alpha particles with energies between 0.6 and 3.4 MeV (protons, deuterons) and 0.9 and 5.4 MeV (alpha particles). In addition, the energy spectrum of ions produced from laser irradiation of thin foils was measured. More detailed studies of the ion generation will be a subject of a separate publication.

ACKNOWLEDGMENTS

The authors wish to express their gratitude to Mark Bedzyk of LLE and Clint Cross and Kurt Fletcher of SUNY Geneseo for their help in the design of the Thomson parabola and for their assistance with the experiments conducted at SUNY Geneseo. This work was supported by the U.S. Department of Energy Office of Inertial Confinement Fusion under Cooperative Agreement No. DE-FC52-08NA28302, the University of Rochester, and the New York State Energy Research and Development Authority.

[1] E. L. Clark, K. Krushelnick, M. Zepf, F. N. Beg, M. Tatarakis, A. Machacek, M. I.K. Santala, I. Watts, P. A. Norreys, and A. E. Dangor, Phys. Rev. Lett. **85**, 1654 (2000).
[2] M. Hegelich, S. Karsch, G. Pretzler, D. Habs, K. Witte, W. Guenther, M. Allen, A. Blazevic, J. Fuchs, J. C. Gauthier, M. Geissel, P. Audebert, T. Cowan, and M. Roth, Phys. Rev. Lett. **89**, 085002 (2002).
[3] M. Mori, M. Kando, A. S. Pirozhkov, Y. Hayashi, A. Yogo, N. Yoshimura, K. Ogura, M. Nishiuchi, A. Sagisaka, S. Orimo, M. Kado, A. Fukumi, Z. Li, S. Nakamura, A. Noda, and D. Hiroyuki, Plasma Fusion Res.**1**, 042 (2006).
[4] W. Mroz, P. Parys, J. Wolowski, E. Woryna, P. Straka, B. Kralikova, J. Krasa, L. Laska, K. Masek, K. Rohlena, T. Mocek, M. Pfeifer, J. Skala, H. Haseroth, J. Collier, B. Y. Sharkov, A. V. Shumshurov, A. V. Golubev, and J. Farny, Rev. Sci. Instrum. **67**, 1272 (1996).
[5] S. S. Medley and A. L. Roquemore, Rev. Sci. Instrum. **69**, 2651 (1998).
[6] V. Bagnoud, I. Begishev, M. J. Guardalben, J. Puth, and J. D. Zuegel, in Proceedings of Conference on Lasers and Electro-Optics/International Quantum Electronics Conference and Photonic Applications Systems Technologies, Optical Society of America, San Francisco, CA, 2004, paper JTuE4.
[7] V. Bagnoud, I. A. Begishev, M. J. Guardalben, J. Puth, and J. D. Zuegel, Opt. Lett. **30**, 1843 (2005).
[8] V. Bagnoud, J. Puth, I. Begishev, M. Guardalben, J. D. Zuegel, N. Forget, C. L. Blanc, and J. Bromage, in Proceedings of Conference on Lasers and Electro-Optics/Quantum Electronics and Laser Science and Photonic Applications Systems Technologies, Optical Society of America, Baltimore, MD, 2005, paper JFA1.
[9] J. J. Thomson, *Proc. R. Soc.*, A **89**, 1 (1913).
[10] S. C. Wilks, A. B. Langdon, T. E. Cowan, M. Roth, M. Singh, S. Hatchett, M. H. Key, D. Pennington, A. MacKinnon, and R. A. Snavely, Phys. Plasmas **8**, 542 (2001).
[11] L. Romagnani, J. Fuchs, M. Borghesi, P. Antici, P. Audebert, F. Ceccherini, T. Cowan, T. Grismayer, S. Kar, A. Macchi, P. Mora, G. Pretzler, A. Schiavi, T. Toncian, and O. Willi, Phys. Rev. Lett. **95**, 195001 (2005).
[12] M. Roth, T. E. Cowan, M. H. Key, S. P. Hatchett, C. Brown, W. Fountain, J. Johnson, D. M. Pennington, R. A. Snavely, S. C. Wilks, K. Yasuike, H. Ruhl, F. Pegoraro, S. V. Bulanov, E. M. Campbell, M. D. Perry, and H. Powell, Phys. Rev. Lett. **86**, 436 (2001).
[13] R. A. Snavely, M. H. Key, S. P. Hatchett, T. E. Cowan, M. Roth, T. W. Phillips, M. A. Stoyer, E. A. Henry, T. C. Sangster, M. S. Singh, S. C. Wilks, A. MacKinnon, A. Offenberger, D. M. Pennington, K. Yasuike, A. B. Langdon, B. F. Lasinski, J. Johnson, M. D. Perry, and E. M. Campbell, Phys. Rev. Lett. **85**, 2945 (2000).
[14] See http://www.dextermag.com/ for information on Dexter permanent magnets.
[15] See http://www.sabic.com/, Ultem is a trademark of SABIC (Saudi Basic Industries Corporation).
[16] See http://www.spellmanhv.com/ for information on the Spellman High Voltage Co., SL series power supply.
[17] See http://www.fujifilm.com/ for information on Fujifilm imaging plates.
[18] A. Nohtomi, T. Terunuma, R. Kohno, Y. Takada, Y. Hayakawa, A. Maruhashi, and T. Sakae, Nucl. Instrum. Methods Phys. Res. A **424**, 569 (1999).
[19] See http://www.pelletron.com/ for information on the S-series Pelletron accelerators.
[20] See http://www.epson.com/ for information on the 10000 XL scanner.
[21] See http://www.fchart.com/feht/ for information on the FEHT software.
[22] J. Pizzonia, Fujifilm Medical Systems USA, Inc., personal communication (2008).
[23] J. F. Ziegler, Nucl. Instrum. Methods Phys. Res. B **219–220**, 1027 (2004).
[24] A. Mancic, J. Fuchs, P. Antici, S. A. Gaillard, and P. Audebert, Rev. Sci. Instrum. **79**, 073301 (2008).
[25] S. Taniguchi, A. Yamadera, T. Nakamura, and A. Fukumura, Nucl. Instrum. Methods Phys. Res. A **413**, 119 (1998).